

## PDF hosted at the Radboud Repository of the Radboud University Nijmegen

The following full text is a preprint version which may differ from the publisher's version.

For additional information about this publication click this link.

<http://hdl.handle.net/2066/124535>

Please be advised that this information was generated on 2017-12-05 and may be subject to change.

# Determination of an Upper Limit for the Mass of the $\tau$ -Neutrino at LEP

The OPAL Collaboration

## Abstract

An upper limit for the  $\nu_\tau$  mass is determined through the kinematic reconstruction of the decay  $\tau \rightarrow 5\pi^\pm\nu_\tau$  in the OPAL detector at LEP. The limit is obtained using a new method based on the comparison of the two-dimensional distribution of energy and invariant mass of the five-pion system with expectations from different neutrino mass hypotheses. From a sample of five events surviving the selection criteria we obtain an upper limit of 74 MeV at 95% confidence level. It is the first measurement at LEP energies, where the larger average multiplicity of  $e^+e^- \rightarrow q\bar{q}$  events makes the suppression of this background more robust compared to lower energies.

(Submitted to Physics Letters B)

# The OPAL Collaboration

R. Akers<sup>16</sup>, G. Alexander<sup>23</sup>, J. Allison<sup>16</sup>, K.J. Anderson<sup>9</sup>, S. Arce<sup>2</sup>, S. Asai<sup>24</sup>, A. Astbury<sup>28</sup>,  
D. Axen<sup>29</sup>, G. Azuelos<sup>18,a</sup>, A.H. Ball<sup>17</sup>, E. Barberio<sup>26</sup>, R.J. Barlow<sup>16</sup>, R. Bartoldus<sup>3</sup>, J.R. Batley<sup>5</sup>,  
G. Beaudoin<sup>18</sup>, A. Beck<sup>23</sup>, G.A. Beck<sup>13</sup>, J. Becker<sup>10</sup>, C. Beeston<sup>16</sup>, T. Behnke<sup>27</sup>, K.W. Bell<sup>20</sup>, G. Bella<sup>23</sup>,  
P. Bentkowsky<sup>18</sup>, S. Bentvelsen<sup>8</sup>, P. Berlich<sup>10</sup>, S. Bethke<sup>32</sup>, O. Biebel<sup>32</sup>, I.J. Bloodworth<sup>1</sup>, P. Bock<sup>11</sup>,  
H.M. Bosch<sup>11</sup>, M. Boutemur<sup>18</sup>, S. Braibant<sup>12</sup>, P. Bright-Thomas<sup>25</sup>, R.M. Brown<sup>20</sup>, A. Buijs<sup>8</sup>,  
H.J. Burckhart<sup>8</sup>, C. Burgard<sup>27</sup>, P. Capiluppi<sup>2</sup>, R.K. Carnegie<sup>6</sup>, A.A. Carter<sup>13</sup>, J.R. Carter<sup>5</sup>,  
C.Y. Chang<sup>17</sup>, C. Charlesworth<sup>6</sup>, D.G. Charlton<sup>8</sup>, S.L. Chu<sup>4</sup>, P.E.L. Clarke<sup>15</sup>, J.C. Clayton<sup>1</sup>,  
S.G. Clowes<sup>16</sup>, I. Cohen<sup>23</sup>, J.E. Conboy<sup>15</sup>, M. Coupland<sup>14</sup>, M. Cuffiani<sup>2</sup>, S. Dado<sup>22</sup>, C. Dallapiccola<sup>17</sup>,  
G.M. Dallavalle<sup>2</sup>, C. Darling<sup>31</sup>, S. De Jong<sup>13</sup>, H. Deng<sup>17</sup>, M. Dittmar<sup>4</sup>, M.S. Dixit<sup>7</sup>, E. do Couto e  
Silva<sup>12</sup>, J.E. Duboscq<sup>8</sup>, E. Duchovni<sup>26</sup>, G. Duckeck<sup>8</sup>, I.P. Duerdoth<sup>16</sup>, U.C. Dunwoody<sup>5</sup>, P.A. Elcombe<sup>5</sup>,  
P.G. Estabrooks<sup>6</sup>, E. Etzion<sup>23</sup>, H.G. Evans<sup>9</sup>, F. Fabbri<sup>2</sup>, B. Fabbro<sup>21</sup>, M. Fanti<sup>2</sup>, M. Fierro<sup>2</sup>,  
M. Fincke-Keeler<sup>28</sup>, H.M. Fischer<sup>3</sup>, P. Fischer<sup>3</sup>, R. Folman<sup>26</sup>, D.G. Fong<sup>17</sup>, M. Foucher<sup>17</sup>, H. Fukui<sup>24</sup>,  
A. Fürtjes<sup>8</sup>, P. Gagnon<sup>6</sup>, A. Gaidot<sup>21</sup>, J.W. Gary<sup>4</sup>, J. Gascon<sup>18</sup>, N.I. Geddes<sup>20</sup>, C. Geich-Gimbel<sup>3</sup>,  
S.W. Gensler<sup>9</sup>, F.X. Gentit<sup>21</sup>, T. Gerasis<sup>20</sup>, G. Giacomelli<sup>2</sup>, P. Giacomelli<sup>4</sup>, R. Giacomelli<sup>2</sup>, V. Gibson<sup>5</sup>,  
W.R. Gibson<sup>13</sup>, J.D. Gillies<sup>20</sup>, J. Goldberg<sup>22</sup>, D.M. Gingrich<sup>30,a</sup>, M.J. Goodrick<sup>5</sup>, W. Gorn<sup>4</sup>,  
C. Grandi<sup>2</sup>, P. Grannis<sup>8</sup>, E. Gross<sup>26</sup>, J. Hagemann<sup>27</sup>, G.G. Hanson<sup>12</sup>, M. Hansroul<sup>8</sup>, C.K. Hargrove<sup>7</sup>,  
J. Hart<sup>8</sup>, P.A. Hart<sup>9</sup>, M. Hauschild<sup>8</sup>, C.M. Hawkes<sup>8</sup>, E. Heflin<sup>4</sup>, R.J. Hemingway<sup>6</sup>, G. Herten<sup>10</sup>,  
R.D. Heuer<sup>8</sup>, J.C. Hill<sup>5</sup>, S.J. Hillier<sup>8</sup>, T. Hilse<sup>10</sup>, D.A. Hinshaw<sup>18</sup>, P.R. Hobson<sup>25</sup>, D. Hochman<sup>26</sup>,  
A. Höcker<sup>3</sup>, R.J. Homer<sup>1</sup>, A.K. Honma<sup>28,a</sup>, R.E. Hughes-Jones<sup>16</sup>, R. Humbert<sup>10</sup>, P. Igo-Kemenes<sup>11</sup>,  
H. Ihssen<sup>11</sup>, D.C. Imrie<sup>25</sup>, A. Jawahery<sup>17</sup>, P.W. Jeffreys<sup>20</sup>, H. Jeremie<sup>18</sup>, M. Jimack<sup>1</sup>, M. Jones<sup>6</sup>,  
R.W.L. Jones<sup>8</sup>, P. Jovanovic<sup>1</sup>, C. Jui<sup>4</sup>, D. Karlen<sup>6</sup>, K. Kawagoe<sup>24</sup>, T. Kawamoto<sup>24</sup>, R.K. Keeler<sup>28</sup>,  
R.G. Kellogg<sup>17</sup>, B.W. Kennedy<sup>20</sup>, B. King<sup>8</sup>, J. King<sup>13</sup>, S. Kluth<sup>5</sup>, T. Kobayashi<sup>24</sup>, M. Kobel<sup>10</sup>,  
D.S. Koetke<sup>8</sup>, T.P. Kokott<sup>3</sup>, S. Komamiya<sup>24</sup>, R. Kowalewski<sup>8</sup>, R. Howard<sup>29</sup>, P. Krieger<sup>6</sup>, J. von  
Krogh<sup>11</sup>, P. Kyberd<sup>13</sup>, G.D. Lafferty<sup>16</sup>, H. Lafoux<sup>8</sup>, R. Lahmann<sup>17</sup>, J. Lauber<sup>8</sup>, J.G. Layter<sup>4</sup>,  
P. Leblanc<sup>18</sup>, P. Le Du<sup>21</sup>, A.M. Lee<sup>31</sup>, E. Lefebvre<sup>18</sup>, M.H. Lehto<sup>15</sup>, D. Lellouch<sup>26</sup>, C. Leroy<sup>18</sup>, J. Letts<sup>4</sup>,  
L. Levinson<sup>26</sup>, Z. Li<sup>12</sup>, F. Liu<sup>29</sup>, S.L. Lloyd<sup>13</sup>, F.K. Loebinger<sup>16</sup>, G.D. Long<sup>17</sup>, B. Lorazo<sup>18</sup>, M.J. Losty<sup>7</sup>,  
X.C. Lou<sup>8</sup>, J. Ludwig<sup>10</sup>, A. Luig<sup>10</sup>, M. Mannelli<sup>8</sup>, S. Marcellini<sup>2</sup>, C. Markus<sup>3</sup>, A.J. Martin<sup>13</sup>,  
J.P. Martin<sup>18</sup>, T. Mashimo<sup>24</sup>, P. Mättig<sup>3</sup>, U. Maur<sup>3</sup>, J. McKenna<sup>29</sup>, T.J. McMahon<sup>1</sup>, A.I. McNab<sup>13</sup>,  
J.R. McNutt<sup>25</sup>, F. Meijers<sup>8</sup>, F.S. Merritt<sup>9</sup>, H. Mes<sup>7</sup>, A. Michelini<sup>8</sup>, R.P. Middleton<sup>20</sup>, G. Mikenberg<sup>26</sup>,  
J. Mildener<sup>6</sup>, D.J. Miller<sup>15</sup>, R. Mir<sup>26</sup>, W. Mohr<sup>10</sup>, C. Moisan<sup>18</sup>, A. Montanari<sup>2</sup>, T. Mori<sup>24</sup>,  
M. Morii<sup>24</sup>, U. Müller<sup>3</sup>, B. Nellen<sup>3</sup>, B. Nijhar<sup>16</sup>, S.W. O'Neale<sup>1</sup>, F.G. Oakham<sup>7</sup>, F. Odoric<sup>2</sup>,  
H.O. Ogren<sup>12</sup>, C.J. Oram<sup>28,a</sup>, M.J. Oreglia<sup>9</sup>, S. Orito<sup>24</sup>, J.P. Pansart<sup>21</sup>, G.N. Patrick<sup>20</sup>, M.J. Pearce<sup>1</sup>,  
P. Pfister<sup>10</sup>, P.D. Phillips<sup>16</sup>, J.E. Pilcher<sup>9</sup>, J. Pinfold<sup>30</sup>, D. Pitman<sup>28</sup>, D.E. Plane<sup>8</sup>, P. Poffenberger<sup>28</sup>,  
B. Poli<sup>2</sup>, A. Posthaus<sup>3</sup>, T.W. Pritchard<sup>13</sup>, H. Przysiezniak<sup>18</sup>, M.W. Redmond<sup>8</sup>, D.L. Rees<sup>8</sup>, D. Rigby<sup>1</sup>,  
M. Rison<sup>5</sup>, S.A. Robins<sup>13</sup>, D. Robinson<sup>5</sup>, J.M. Roney<sup>28</sup>, E. Ros<sup>8</sup>, S. Rossberg<sup>10</sup>, A.M. Rossi<sup>2</sup>,  
M. Rosvick<sup>28</sup>, P. Routenburg<sup>30</sup>, Y. Rozen<sup>8</sup>, K. Runge<sup>10</sup>, O. Runolfsson<sup>8</sup>, D.R. Rust<sup>12</sup>, M. Sasaki<sup>24</sup>,  
C. Sbarra<sup>2</sup>, A.D. Schaile<sup>8</sup>, O. Schaile<sup>10</sup>, F. Scharf<sup>3</sup>, P. Scharff-Hansen<sup>8</sup>, P. Schenk<sup>4</sup>, B. Schmitt<sup>3</sup>, H. von  
der Schmitt<sup>11</sup>, M. Schröder<sup>12</sup>, H.C. Schultz-Coulon<sup>10</sup>, P. Schütz<sup>3</sup>, M. Schulz<sup>8</sup>, C. Schwick<sup>27</sup>,  
J. Schwiening<sup>3</sup>, W.G. Scott<sup>20</sup>, M. Settles<sup>12</sup>, T.G. Shears<sup>5</sup>, B.C. Shen<sup>4</sup>, C.H. Shepherd-Themistocleous<sup>7</sup>,  
P. Sherwood<sup>15</sup>, G.P. Sioli<sup>2</sup>, A. Skillman<sup>16</sup>, A. Skuja<sup>17</sup>, A.M. Smith<sup>8</sup>, T.J. Smith<sup>28</sup>, G.A. Snow<sup>17</sup>,  
R. Sobie<sup>28</sup>, R.W. Springer<sup>17</sup>, M. Sproston<sup>20</sup>, A. Stahl<sup>3</sup>, C. Stegmann<sup>10</sup>, K. Stephens<sup>16</sup>, J. Steuerer<sup>28</sup>,  
B. Stockhausen<sup>3</sup>, R. Ströhmer<sup>11</sup>, D. Strom<sup>19</sup>, P. Szymanski<sup>20</sup>, H. Takeda<sup>24</sup>, T. Takeshita<sup>24</sup>, S. Tarem<sup>26</sup>,  
M. Tecchio<sup>9</sup>, P. Teixeira-Dias<sup>11</sup>, N. Tesch<sup>3</sup>, M.A. Thomson<sup>15</sup>, S. Towers<sup>6</sup>, T. Tsukamoto<sup>24</sup>,  
M.F. Turner-Watson<sup>8</sup>, D. Van den plas<sup>18</sup>, R. Van Kooten<sup>12</sup>, G. Vasseur<sup>21</sup>, M. Vincker<sup>28</sup>, A. Wagner<sup>27</sup>,  
D.L. Wagner<sup>9</sup>, C.P. Ward<sup>5</sup>, D.R. Ward<sup>5</sup>, J.J. Ward<sup>15</sup>, P.M. Watkins<sup>1</sup>, A.T. Watson<sup>1</sup>, N.K. Watson<sup>7</sup>,  
P. Weber<sup>6</sup>, P.S. Wells<sup>8</sup>, N. Wermes<sup>3</sup>, B. Wilkens<sup>10</sup>, G.W. Wilson<sup>4</sup>, J.A. Wilson<sup>1</sup>, V-H. Winterer<sup>10</sup>,  
T. Wlodek<sup>26</sup>, G. Wolf<sup>26</sup>, S. Wotton<sup>11</sup>, T.R. Wyatt<sup>16</sup>, A. Yeaman<sup>13</sup>, G. Yekutieli<sup>26</sup>, M. Yurko<sup>18</sup>,  
W. Zeuner<sup>8</sup>, G.T. Zorn<sup>17</sup>.

- <sup>1</sup>School of Physics and Space Research, University of Birmingham, Birmingham B15 2TT, UK
- <sup>2</sup>Dipartimento di Fisica dell' Università di Bologna and INFN, I-40126 Bologna, Italy
- <sup>3</sup>Physikalisches Institut, Universität Bonn, D-53115 Bonn, Germany
- <sup>4</sup>Department of Physics, University of California, Riverside CA 92521, USA
- <sup>5</sup>Cavendish Laboratory, Cambridge CB3 0HE, UK
- <sup>6</sup>Carleton University, Department of Physics, Colonel By Drive, Ottawa, Ontario K1S 5B6, Canada
- <sup>7</sup>Centre for Research in Particle Physics, Carleton University, Ottawa, Ontario K1S 5B6, Canada
- <sup>8</sup>CERN, European Organisation for Particle Physics, CH-1211 Geneva 23, Switzerland
- <sup>9</sup>Enrico Fermi Institute and Department of Physics, University of Chicago, Chicago IL 60637, USA
- <sup>10</sup>Fakultät für Physik, Albert Ludwigs Universität, D-79104 Freiburg, Germany
- <sup>11</sup>Physikalisches Institut, Universität Heidelberg, D-69120 Heidelberg, Germany
- <sup>12</sup>Indiana University, Department of Physics, Swain Hall West 117, Bloomington IN 47405, USA
- <sup>13</sup>Queen Mary and Westfield College, University of London, London E1 4NS, UK
- <sup>14</sup>Birkbeck College, London WC1E 7HV, UK
- <sup>15</sup>University College London, London WC1E 6BT, UK
- <sup>16</sup>Department of Physics, Schuster Laboratory, The University, Manchester M13 9PL, UK
- <sup>17</sup>Department of Physics, University of Maryland, College Park, MD 20742, USA
- <sup>18</sup>Laboratoire de Physique Nucléaire, Université de Montréal, Montréal, Quebec H3C 3J7, Canada
- <sup>19</sup>University of Oregon, Department of Physics, Eugene OR 97403, USA
- <sup>20</sup>Rutherford Appleton Laboratory, Chilton, Didcot, Oxfordshire OX11 0QX, UK
- <sup>21</sup>CEA, DAPNIA/SPP, CE-Saclay, F-91191 Gif-sur-Yvette, France
- <sup>22</sup>Department of Physics, Technion-Israel Institute of Technology, Haifa 32000, Israel
- <sup>23</sup>Department of Physics and Astronomy, Tel Aviv University, Tel Aviv 69978, Israel
- <sup>24</sup>International Centre for Elementary Particle Physics and Department of Physics, University of Tokyo, Tokyo 113, and Kobe University, Kobe 657, Japan
- <sup>25</sup>Brunel University, Uxbridge, Middlesex UB8 3PH, UK
- <sup>26</sup>Particle Physics Department, Weizmann Institute of Science, Rehovot 76100, Israel
- <sup>27</sup>Universität Hamburg/DESY, II Institut für Experimental Physik, Notkestrasse 85, D-22607 Hamburg, Germany
- <sup>28</sup>University of Victoria, Department of Physics, P O Box 3055, Victoria BC V8W 3P6, Canada
- <sup>29</sup>University of British Columbia, Department of Physics, Vancouver BC V6T 1Z1, Canada
- <sup>30</sup>University of Alberta, Department of Physics, Edmonton AB T6G 2J1, Canada
- <sup>31</sup>Duke University, Dept of Physics, Durham, NC 27708-0305, USA
- <sup>32</sup>Technische Hochschule Aachen, III Physikalisches Institut, Sommerfeldstrasse 26-28, D-52056 Aachen, Germany

<sup>a</sup>Also at TRIUMF, Vancouver, Canada V6T 2A3

# 1 Introduction

Massive neutrinos have been proposed as possible explanations for a variety of outstanding problems in particle physics and astrophysics, including the ‘dark matter’ problem of the universe, the solar neutrino problem, and in various extensions of the Standard Model of electroweak interactions.

Existing upper limits on the  $\nu_\tau$  mass have been derived from studies of the invariant mass spectra of high mass multi-pion decays of the  $\tau$  lepton. At present the best limits are 31 MeV at 95% confidence level (c.l.) obtained by the ARGUS collaboration [1] from studies of the  $\tau \rightarrow 5\pi^\pm\nu_\tau$  decay and 32.6 MeV at 95% c.l. by the CLEO collaboration [2] using a combined analysis of the  $\tau \rightarrow 5\pi^\pm\nu_\tau$  and  $\tau \rightarrow 3\pi^\pm 2\pi^0\nu_\tau$  decays. Although the kinematics of  $\tau$  decay mean that measurements of the  $\nu_\tau$  mass are well performed at low energies, near the  $\tau$  pair production threshold, the measurements at high energy possible at LEP have the advantage that their background conditions are different; in particular the background from multi-hadron events ( $e^+e^- \rightarrow q\bar{q}$ ) is much smaller. This is due to the fact that the multiplicity of charged tracks and their topology allow a cleaner separation between the signal  $\tau$ -pair events and the background from multi-hadron events. The multiplicity of  $e^+e^- \rightarrow q\bar{q}$  events scales logarithmically with the center of mass energy whereas the multiplicity of  $\tau$  decays remains constant.

We present in this paper the first determination of an upper limit for  $m_{\nu_\tau}$  from LEP data which, for the reasons given above, we consider as an important independent measurement compared to earlier results [1] [2] obtained at lower energies. We also employ here, for the first time, a two-dimensional method [3] using the invariant mass and total energy of the charged hadrons of the decay  $\tau \rightarrow 5\pi^\pm\nu_\tau$ . In a simple form the method is represented by the two inequalities

$$m_{\nu_\tau} \leq m_\tau - m_X$$

$$m_{\nu_\tau} \leq E_\tau - E_X,$$

where  $E_X$  is the energy of the charged hadrons and  $m_X$  their invariant mass. The kinematically allowed region in the  $m - E$  space for  $\tau$  decays is shown in Fig. 1 for two different  $\nu_\tau$  masses. Better discrimination between the different  $m_{\nu_\tau}$  hypotheses is achieved by exploiting the distribution of invariant mass and energy of the  $\tau$  decay rather than just using the one-dimensional missing mass method which integrates over the energy dependence. From Fig. 1 it is evident that the limit on the neutrino mass is dominated by the events in the kinematically sensitive region close to  $E_\tau$  and  $m_\tau$ . Events far from the boundary show no sensitivity to  $m_{\nu_\tau}$ . Further details of the analysis can be found in [4].

The analysis presented here is based on data taken with the OPAL detector during 1992. The total integrated luminosity amounts to  $24.5 \text{ pb}^{-1}$  which gives an expected sample of about 36 000  $\tau^+\tau^-$  events. Because the silicon microvertex detector installed in summer 1991 plays an important role in the analysis, data taken prior to 1992 were not used. A detailed description of the OPAL detector can be found elsewhere [5]. We present here the characteristics relevant for this analysis. The 1992 silicon microvertex detector [6] consists of two layers of single-sided silicon strip detectors with 11 inner sectors located at a radius of 61 mm with respect to the nominal beam line and 14 outer sectors at 75 mm. The readout pitch is  $50 \mu\text{m}$  and the achieved impact parameter resolution derived from dilepton data is about  $15 \mu\text{m}$  in the plane perpendicular to the beam axis. Apart from the silicon microvertex detector, this analysis uses the vertex and central drift chambers, the outer z-measuring chambers<sup>1</sup> and the electromagnetic calorimeter. The achieved average double-hit resolution of the central jet chamber is 2.2 mm. The momentum resolution of isolated tracks is  $\sigma_p/p = \sqrt{(0.02)^2 + (0.0015 \cdot p [\text{GeV}])^2}$  and

---

<sup>1</sup>where  $z$  is the direction of the beam.

the  $dE/dx$  resolution  $\frac{\sigma(dE/dx)}{dE/dx} = 3.5\%$  for minimum ionising pions in jets with the maximum number of hits (159), resulting in a  $\pi$ - $e$  separation of at least  $2\sigma$  up to momenta of 18 GeV. More details of the performance of this detector can be found in [7] and [8].

## 2 Selection of $\tau \rightarrow 5\pi^\pm\nu_\tau$

At LEP,  $\tau^+\tau^-$  events have the distinctive signature of two back-to-back jets where the charged tracks are highly collimated due to the large Lorentz boost. It is thus convenient to group the charged tracks and clusters in the electromagnetic calorimeter into cones of half angle  $35^\circ$ . We select  $\tau^+\tau^-$  events with exactly two cones in which at least one charged track per cone must exceed 1% of the beam energy. Events which have either a charged track or an unassociated electromagnetic cluster outside the two cones are removed. Background coming from two photon events and events with initial state radiation are removed by requiring an acolinearity angle of less than  $10^\circ$  between the two cones.

A  $\tau \rightarrow 5\pi^\pm\nu_\tau$  candidate must have exactly five charged tracks in one cone balanced by a  $\tau$  candidate with one or three charged tracks in the opposite ('recoil') cone (5-1 or 5-3 topology). Charged tracks to be used in the analysis are required to have  $p_T > 100$  MeV,  $|d_0| < 2$  cm,  $|z_0| < 75$  cm,  $R_{min} < 75$  cm and  $N > 40$ . Here  $p_T$  is the transverse momentum relative to the beam direction,  $|d_0|$  is the two-dimensional impact parameter,  $z_0$  is the  $z$ -coordinate at the point of closest approach to the interaction vertex,  $R_{min}$  is the radius in the  $x$ - $y$  plane of the first measured point in the jet chamber and  $N$  is the number of measured space points in the jet chamber. The total charge of each cone must be  $\pm 1$  adding up to a total event charge of zero. The pion mass is assumed for conversion of momentum into energy.

The two most serious background reactions remaining after these relatively loose selection criteria are from  $e^+e^- \rightarrow q\bar{q}$  and from  $\tau$  decays with photon conversions (e.g.  $\tau \rightarrow 3\pi^\pm \geq 1\pi^0, \pi^0 \rightarrow \gamma\gamma$ ). The invariant mass and energy of multi-hadron events are not limited by  $\tau$  decay kinematics and thus can be spread over the entire area of Fig. 1. However an accidental event at the kinematic boundary would mimic a very low neutrino mass. Tau decays with conversions are dangerous because misidentification of the electrons as pions leads to an overestimate of  $m_X$  which results in an underestimate of the neutrino mass. The selection criteria are optimized to achieve a  $\tau \rightarrow 5\pi^\pm\nu_\tau$  sample with minimal backgrounds from these sources. Some events from the decay  $\tau \rightarrow 5\pi^\pm\pi^0\nu_\tau$  survive the cuts, but this does not affect our neutrino mass limit, as will be discussed in the next section.

The first set of cuts exploits the fact that all five charged tracks must be pions in the  $\tau \rightarrow 5\pi^\pm\nu_\tau$  decay. We require that the fraction  $E/p$  must be smaller than 0.6, where  $E$  is the deposited energy in the electromagnetic calorimeter in the cone and  $p$  is the sum over the momenta of the five charged tracks. The cone itself is used here because the charged tracks are often so close together that an analysis of the  $E/p$  fraction for single tracks is impossible since the clusters are merged together. Candidates for a  $\tau \rightarrow 5\pi^\pm\nu_\tau$  decay with one or more electrons clearly identified by the  $dE/dx$  measurement ( $\ln(P(e)/P(\pi)) > 5.5$ ) are removed. Here  $P(\pi)$  ( $P(e)$ ) is the  $\chi^2$ -probability that the track is consistent with the pion (electron) hypothesis derived from the  $dE/dx$  and momentum measurements. In addition a likelihood comparison of a final state to be five pions or three pions and two electrons is performed. The fraction  $\frac{P(5\pi)}{P(5\pi)+P(3\pi 2e)}$  must be larger than 0.9 with  $P(5\pi) = \prod_{i=1}^5 P_i(\pi)$  and  $P(3\pi 2e)$  summing up the combinatorial possibilities of three particles to be pions and two to be oppositely charged electrons.

The second group of cuts uses the fact that all five charged tracks must come from one common

vertex, compatible with the average flight distance of a  $\tau$  lepton (2.2 mm at LEP energies). Events where any of the tracks has an impact parameter larger than 0.9 mm are rejected. After these cuts a three dimensional refit of all tracks to a common vertex is performed. Only events with a  $\chi^2$ -probability larger than 5% for this fit are accepted. Events with a fitted decay length of more than 2 cm in the  $x$ - $y$  plane ( $z$  is the direction of the beam) and more than 10 cm in three dimensions are removed. In addition, using the refitted track parameters improves the mass resolution by up to a factor of two.

Eight candidate events remain after applying the selection cuts to the 1992 data sample. As shown in the central column of Table 1 five events have a 5-1 topology, three candidates have a 5-3 topology.

### 3 Background Estimation

The estimate of the background from  $\tau$  decays with final state photon conversions is made using Monte Carlo events. The selection cuts are applied to a sample of 300 000  $\tau^+\tau^-$  events (roughly 8 times the size of the data sample) with full detector simulation [9]. The events were generated using the KORALZ 3.8 program [10] which describes  $\tau^+\tau^-$  production and the TAUOLA 1.5 program [11] which describes  $\tau$  decay. No background events pass our selection cuts. A background of less than 0.14 events at 68% c.l. is therefore deduced. We have verified that the Monte Carlo simulation describes the data well in all distributions used for the event selection.

The background from  $e^+e^- \rightarrow q\bar{q}$  events can be estimated from the full data sample. The high average charged multiplicity of multi-hadron events (21.3 at LEP energies [12]) makes it unlikely that an  $e^+e^- \rightarrow q\bar{q}$  event has a 5-1 or 5-3 topology as demanded for the signal channel. The expected contamination is derived by tagging multi-hadron events, requiring six or more charged tracks in one cone, examining the charged multiplicity of the recoil cone and extrapolating to the topologies of interest. Selection of such events resembles that for the signal channel but particle identification,  $E/p$  and vertex cuts are removed. These events are corrected for the expected contribution from  $\tau$  decays predicted by the Monte Carlo. Correlation effects between the multiplicities of the cones arising from the flavour of the primary quarks or from kinematic effects are negligible. However, we take into account a small correlation arising from the fact that events are produced with zero net charge. The multiplicity distribution for the recoil cone in the tagged multi-hadron events is normalized to those signal events which have passed all selection criteria except for the requirement for the number of charged tracks in the recoil cone. This normalization is done using the zero events found in the 5-2 and 5-4 topology bins, making the conservative assumption that these bins are populated only by multi-hadron events. An upper limit for the multi-hadron background can be obtained by extrapolating the observed charged multiplicity distribution of multi-hadron events from the appropriate Poisson errors of the 5-2 and 5-4 bins to the signal topologies 5-1 and 5-3 (see Fig. 2). As shown in Table 1 this yields an expected multi-hadron background of less than 0.09 events at 68% c.l. in the 5-1 topology and less than 0.58 events in the 5-3 topology. Because the method employed in this analysis relies greatly on a true background-free sample, the 5-3 topologies are not considered any further in this analysis.

| topology | number of events | upper limit for multi-hadron events |
|----------|------------------|-------------------------------------|
| 5-1      | 5                | 0.09                                |
| 5-2      | 0                | 0.25                                |
| 5-3      | 3                | 0.58                                |
| 5-4      | 0                | 0.87                                |

Table 1: *Number of events selected for various topologies. The central column describes the number of ('signal') events found after applying all selection cuts while the right column lists the upper limit for multi-hadron events normalized to data as described in the text.*

## 4 Results

The five selected  $\tau \rightarrow 5\pi^\pm\nu_\tau$  candidates with 5-1 topology are shown in Fig. 1. It is evident that the event with the highest invariant mass ('best event') dominates the determination of the  $\nu_\tau$  mass. Two events show some sensitivity resulting from their energy information. The two remaining events give little information on  $m_{\nu_\tau}$ .

Because of the strong dependence of the limit on  $m_{\nu_\tau}$  on an individual event (calculating the limit without this 'best event' yields about twice the finally achieved  $m_{\nu_\tau}$  limit) the 'best event' has been intensively studied. It has an invariant mass of  $1.731 \pm 0.023$  GeV and a total energy of  $43.03 \pm 0.81$  GeV. The 'best event' is very well reconstructed by the OPAL detector. All five charged tracks have the maximum number of available hits in the z-chambers located just outside the central jet chamber. Both layers of the silicon microvertex detector show five well separated hits matching well with the extrapolation of the five charged tracks (see Fig. 3). While this fact by itself does not prove the five-pion composition of this decay, it supports the interpretation because five well separated tracks are not likely to contain a photon conversion in the silicon itself nor in the 1.1 mm thick beryllium inner beam pipe located 8 mm before the inner silicon layer. In addition the  $dE/dx$  measurement strongly supports the five pion hypotheses. The ratio previously defined for five pions compared to three pions plus two electrons is 0.985. Assuming two unlike-sign tracks to be electrons, the lowest invariant mass is 151 MeV. The recoil side shows a clear muon track with momentum  $p = 7.96$  GeV with associated hits in the corresponding muon chambers (see Fig. 3). The recoil cone is identified by our standard  $\tau$  selection [13] as a  $\tau \rightarrow \mu\bar{\nu}_\mu\nu_\tau$  decay which is an additional indication that this event is not due to multi-hadron background. These studies show that the probability of the 'best event' being due to background is extremely small.

Recent measurements from the CLEO Collaboration [14] showed that the branching ratio for the decay  $\tau \rightarrow 5\pi^\pm\nu_\tau$  is about four times greater than for the  $\tau \rightarrow 5\pi^\pm\pi^0\nu_\tau$  channel. These channels are difficult to distinguish because the two photons from the  $\pi^0 \rightarrow \gamma\gamma$  decay are often merged into the clusters of the charged tracks. The demand for exactly five charged tracks, which excludes events where one of the photons converts, and the cut on  $E/p < 0.6$  suppress  $\tau \rightarrow 5\pi^\pm\pi^0\nu_\tau$  decays by another factor of two compared to  $\tau \rightarrow 5\pi^\pm\nu_\tau$  decays. The average efficiencies are 4.2% for the  $\tau \rightarrow 5\pi^\pm\nu_\tau$  decay and 2.4% for the  $\tau \rightarrow 5\pi^\pm\pi^0\nu_\tau$  channel. Misidentification of a  $\tau \rightarrow 5\pi^\pm\pi^0\nu_\tau$  decay would reduce the energy and the invariant mass of the final state at least by 135 MeV due to the omission of the  $\pi^0$ . The reduction of the invariant mass for the  $\tau \rightarrow 5\pi^\pm\pi^0\nu_\tau$  events shifts an event away from the boundary in Fig. 1 and thus will always tend to weaken the upper limit for  $m_{\nu_\tau}$ . The downward shift in the energy could potentially yield an event near the lower kinematic boundary in Fig. 1, but for the data events observed this does not affect our limit. The 'best event' in particular does not permit a  $5\pi^\pm\pi^0$  interpretation since its invariant mass is so close to  $m_\tau$ .



An upper limit on the  $\tau$ -neutrino mass is obtained from a likelihood analysis. A probability for every selected event  $i$  is calculated by convolving the theoretical prediction with the experimental resolution  $R$  and the detection efficiency  $\epsilon$

$$P_i(m_\nu, m_i, E_i) = \frac{\int dm \int dE \frac{d^2\Gamma(m_\nu, m, E)}{dm dE} R(m - m_i, E - E_i, \sigma_{m_i}, \sigma_{E_i}) \epsilon(m, E)}{\int dm \int dE \frac{d^2\Gamma(m_\nu, m, E)}{dm dE} \epsilon(m, E)}.$$

The theoretical prediction  $\frac{d^2\Gamma(m_\nu, m, E)}{dm dE}$  is generated as a function of the neutrino mass using KORALZ / TAUOLA including initial state radiation. The neutrino mass was restricted to the physical values of  $m_{\nu_\tau} \geq 0$ . The theoretical prediction employs the new value of  $1777.0 \pm 0.3$  MeV [15] for the  $\tau$  mass. The detection efficiency  $\epsilon(m, E)$  is derived from Monte Carlo events with full detector simulation [9]. It shows no significant dependence on the invariant mass and energy.

Because of the strong dependence of the experimental resolution  $R(m - m_i, E - E_i, \sigma_{m_i}, \sigma_{E_i})$  on the properties of specific events (i.e. number of  $z$ -chamber hits or number of silicon-microvertex detector hits) the resolution is determined individually for each of the five data events. The measured four momenta of each of the five selected events are passed several hundred times through the detector simulation [9] and are reconstructed again. Those events that have the same or slightly worse quality of reconstruction as the original data event are used to determine the experimental resolution by fitting a two-dimensional Gaussian function with correlation in an unbinned likelihood fit to the invariant mass and energy spectrum of the simulated events. The result of these fits is shown by the error ellipses in Fig. 1. We have verified that the quoted limit is insensitive, to the level of 2–3 MeV, to the known discrepancies between the performance of the real detector and that simulated in the Monte Carlo.

The upper limit for  $m_{\nu_\tau}$  at 95% c.l. is calculated from the combined likelihood of the five events which have passed the  $\tau \rightarrow 5\pi^\pm\nu_\tau$  identification. The distribution of the combined likelihood falls continuously with increasing neutrino mass. For the most probable value we find  $m_{\nu_\tau} = 0$  and obtain an upper limit at 95% c.l. of

$$m_{\nu_\tau} < 74 \text{ MeV}.$$

Deriving the upper limit for the  $\tau$ -neutrino mass from only the ‘best event’ yields 77 MeV (at 95% c.l.).

## 5 Conclusion

An upper limit for the mass of the  $\tau$ -neutrino of 74 MeV at 95% c.l. has been obtained using, for the first time, a two-dimensional method based on the invariant mass and the energy of the charged hadrons of the decay  $\tau \rightarrow 5\pi^\pm\nu_\tau$ . It is the first measurement at LEP energies, where the larger average multiplicity of  $e^+e^- \rightarrow q\bar{q}$  events makes the suppression of this background more robust compared to lower energies.

## 6 Acknowledgements

We gratefully acknowledge stimulating discussions and advice from Johannes Raab. It is a pleasure to thank the SL Division for the efficient operation of the LEP accelerator, the precise information on

the absolute energy, and their continuing close cooperation with our experimental group. In addition to the support staff at our own institutions we are pleased to acknowledge the  
Department of Energy, USA,  
National Science Foundation, USA,  
Particle Physics and Astronomy Research Council, UK,  
Natural Sciences and Engineering Research Council, Canada,  
Fussefeld Foundation,  
Israel Ministry of Science,  
Israel Science Foundation, administered by the Israel Academy of Science and Humanities,  
Minerva Gesellschaft,  
Japanese Ministry of Education, Science and Culture (the Monbusho) and a grant under the Monbusho International Science Research Program,  
German Israeli Bi-national Science Foundation (GIF),  
Direction des Sciences de la Matière du Commissariat à l'Énergie Atomique, France,  
Bundesministerium für Forschung und Technologie, Germany,  
National Research Council of Canada,  
A.P. Sloan Foundation and Junta Nacional de Investigação Científica e Tecnológica, Portugal.

## References

- [1] ARGUS Collaboration, H. Albrecht et al., *Phys. Lett.* **B202** (1988) 149 ;  
ARGUS Collaboration, H. Albrecht et al., *Phys. Lett.* **B292** (1992) 221.
- [2] CLEO Collaboration, D. Cinabro et al., *Phys. Rev. Lett.* **70** (1993) 3700.
- [3] Johannes Raab, who first suggested this method, *private communication*.
- [4] A. Posthaus, *Thesis University Bonn IB 94-03* (1994).
- [5] OPAL Collaboration, K. Ahmet et al., *Nucl. Inst. and Meth.* **A305** (1991) 275.
- [6] P. P. Allport et al., *Nucl. Inst. and Meth.* **A324** (1993) 34.
- [7] O. Biebel et al., *Nucl. Inst. and Meth.* **A323** (1992) 169.
- [8] M. Hauschild et. al., *Nucl. Inst. and Meth.* **A314** (1992) 74.
- [9] J. Allison et al., *Nucl. Inst. and Meth.* **A317** (1992) 47.
- [10] S. Jadach, B. F. Ward und Z. Was, *Comp. Phys. Comm.* **66** (1991) 276.
- [11] S. Jadach, J. H. Kühn und Z. Was, *Comp. Phys. Comm.* **64** (1991) 275.
- [12] OPAL Collaboration, M. Z. Akrawy et al., *Z. Phys.* **C47** (1990) 505.
- [13] OPAL Collaboration, G. Alexander et. al., *Phys. Lett.* **B266** (1991) 201.
- [14] CLEO Collaboration, D. Gibaut et al., *CLNS 94/1284 CLEO 94-12*.
- [15] Particle Data Group, K. Hikasa et al. *Phys. Rev.* **D45** (1992) ;  
BES Collaboration, J. Z. Bai et al. *Phys. Rev. Lett.* **69** (1992) 3021 ;  
CLEO Collaboration, R. Balest et al. *Phys. Rev.* **D47** (1993) R3671 ;  
ARGUS Collaboration, H. Albrecht et al. *Phys. Lett.* **B292** (1992) 221.

## 7 Figure Captions

**Figure 1:** Selected  $\tau \rightarrow 5\pi^\pm\nu_\tau$  data events with their respective  $1\sigma$  error ellipses indicating the experimental resolution. The Monte Carlo prediction for reconstructed  $\tau \rightarrow 5\pi^\pm\nu_\tau$  events which are required to pass all selection criteria is plotted as hatched boxes. The events are generated with zero neutrino mass. The area of the boxes corresponds to the number of entries. The Monte Carlo statistics are about eight times the expected number of data events. The lines show the kinematically allowed ranges for  $m_{\nu_\tau} = 0$  and  $m_{\nu_\tau} = 100$  MeV. Monte Carlo events lying outside the kinematically allowed region result from statistical fluctuations due to the experimental resolution of these events and from energy loss due to initial state radiation.

**Figure 2:** Extrapolation of the multi-hadron background into the region of the data events which have passed the  $\tau \rightarrow 5\pi^\pm\nu_\tau$  identification. The dots represent the selected data events showing the expected behaviour of  $\tau$  decays with no entries at even numbers of tracks. The stars represent the upper limit for multi-hadron background normalized to the Poisson errors of these even-track bins.

**Figure 3:** (top)  $x$ - $y$  view of the event with the highest invariant  $5\pi^\pm$  mass. The deposited energy is displayed as boxes which are proportional to the amount of energy. The muon chamber signal is marked as an arrow. Charged tracks are shown as solid lines.  
(bottom) Detailed section of the same event near the silicon-microvertex detector. The charged tracks are shown with their respective hits.

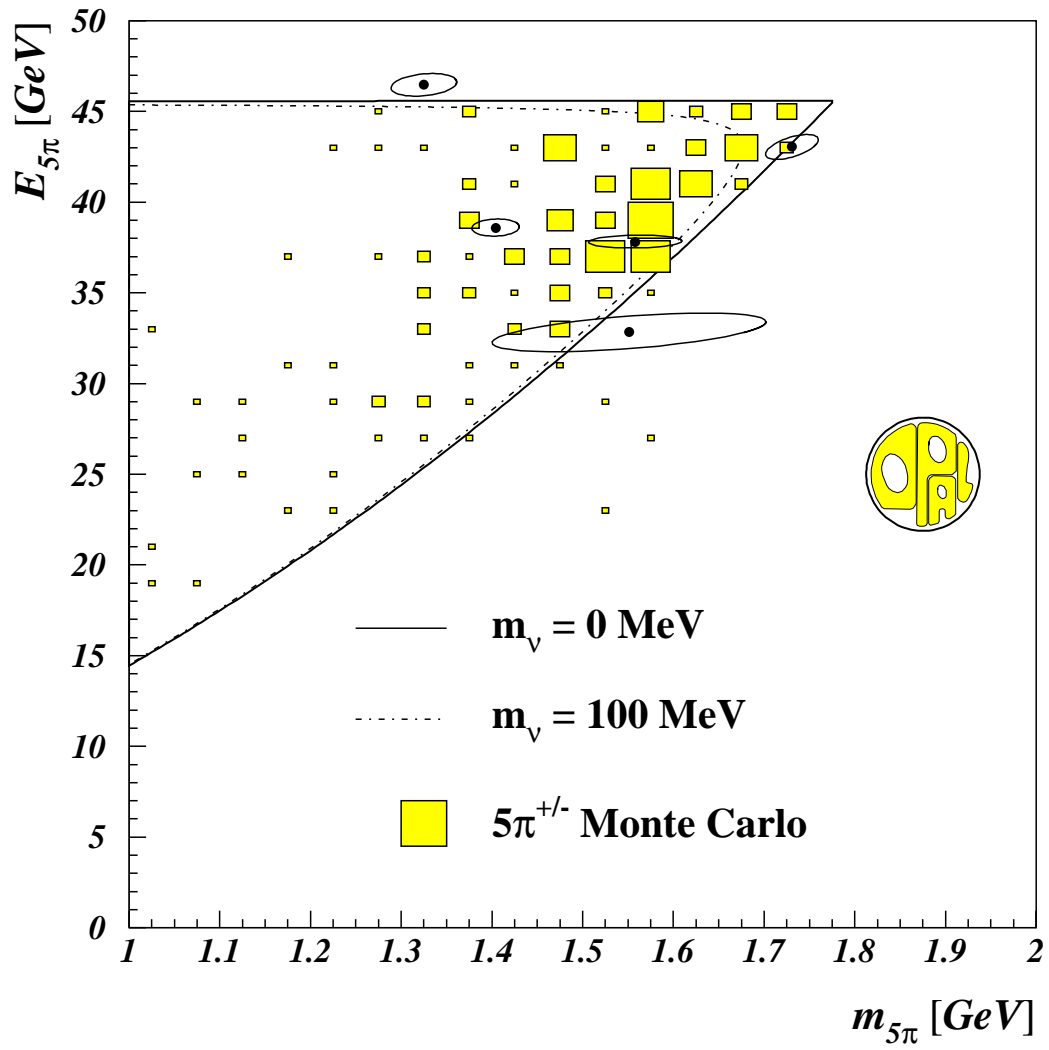


Figure 1:

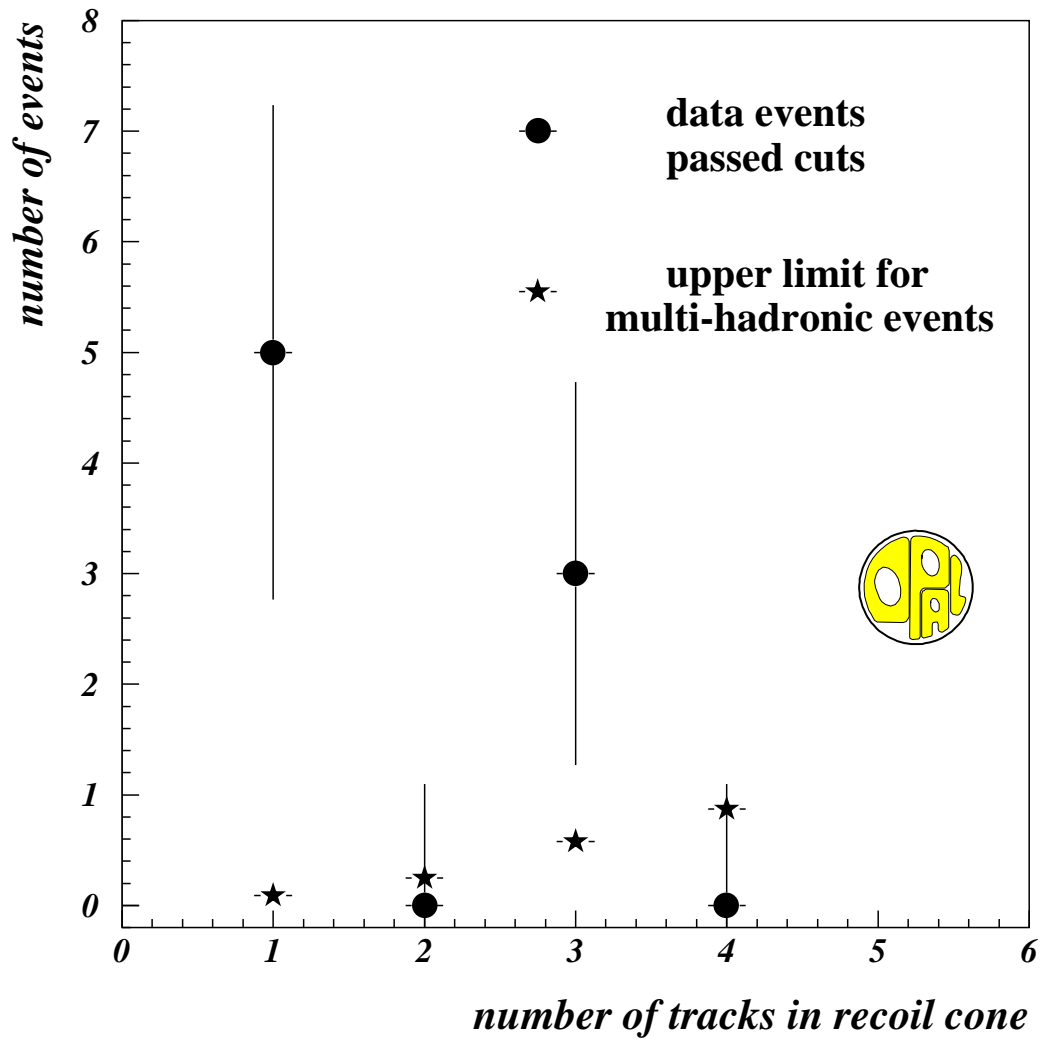


Figure 2:

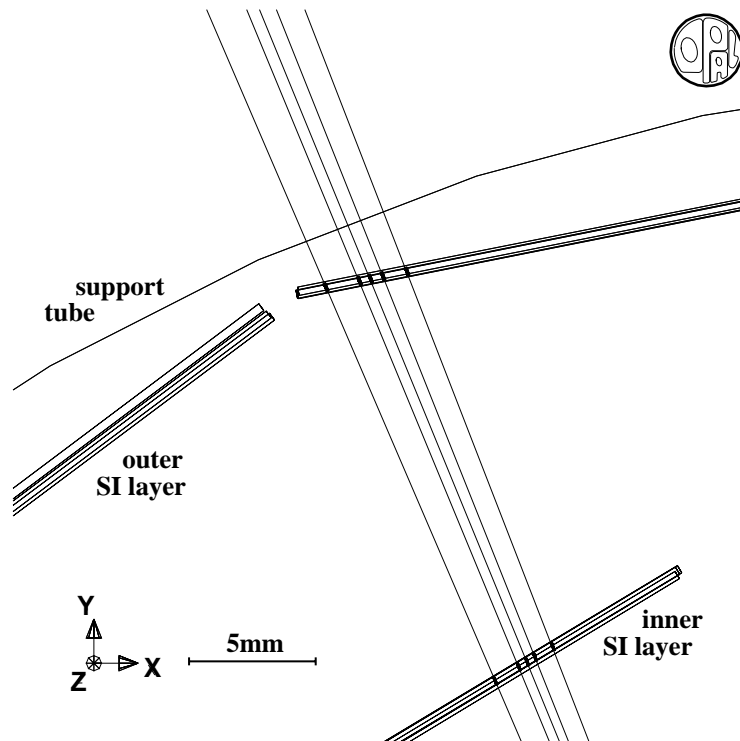
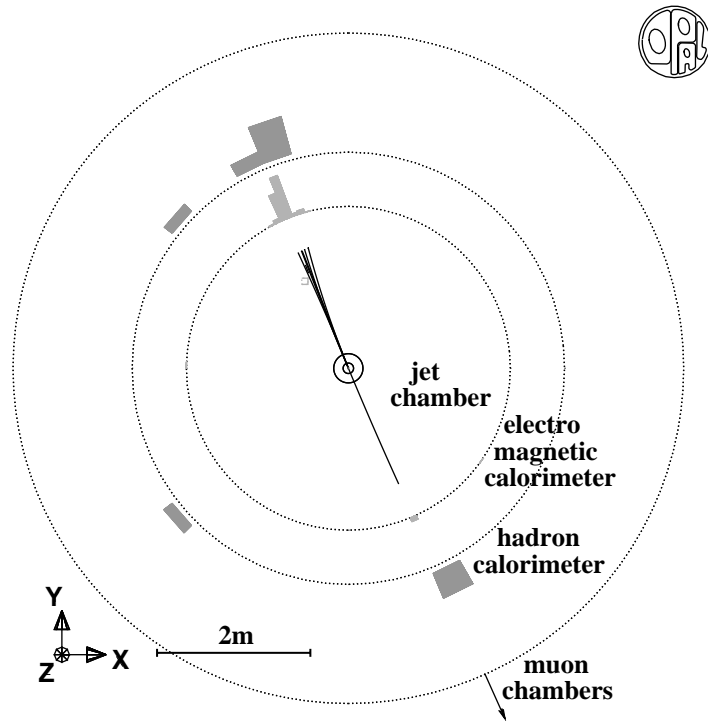


Figure 3: